Polyhedron 75 (2014) 110–117

Contents lists available at ScienceDirect

Polyhedron

journal homepage: www.elsevier.com/locate/poly

Synthesis, characterization and structural comparisons of phosphonium and arsenic dithiocarbamates with alkyl and phenyl substituents

Courtney M. Donahue [a], Isabella K. Black [a], Samantha L. Pecnik [a], Thomas R. Savage [a], Brian L. Scott [b], Scott R. Daly [a,*]

[a] The George Washington University, Department of Chemistry, 725 21st St., NW Washington, DC 20052, USA
[b] Los Alamos National Laboratory, Los Alamos, NM 87545, USA

ARTICLE INFO

Article history:
Received 25 November 2013
Accepted 6 March 2014
Available online 19 March 2014

Keywords:
Dithiocarbamates
Arsenic
Phosphonium
Crystal structure
X-ray diffraction
Sulfur ligand

ABSTRACT

The synthesis and characterization of the new arsenic dithiocarbamate complex $As[S_2CNPh_2]_3$ and three new phosphonium dithiocarbamates $[PPh_4][S_2CNR_2]$, where $R_2 = Et_2$, $(CH_2)_5$ and Ph_2, are reported. $As[S_2CNPh_2]_3$ was prepared by treating AsI_3 with three equivalents of NaS_2CNPh_2 in a 2:1 mixture of H_2O and EtOH. The precipitate that formed was recrystallized from hot toluene to yield yellow prisms of $As[S_2CNPh_2]_3$ suitable for single-crystal X-ray diffraction (XRD). Attempts to prepare the known compound $As[S_2CN(CH_2)_5]_3$ using a similar route resulted in a mixture of $As[S_2CN(CH_2)_5]_3$ and the mixed iodide species $As[S_2CN(CH_2)_5]_2I$. Single-crystals of both compounds were isolated from concentrated $Et_2O/CHCl_3$ solutions and their structures are described here for the first time. $[PPh_4][S_2CNR_2]$ salts were prepared for comparison to arsenic dithiocarbamates by metathesis reactions with PPh_4Br and NaS_2CNR_2 in acetonitrile. All three salts could be obtained in high-purity from $MeCN/Et_2O$ solutions and crystal structures of $[PPh_4][S_2CNEt_2]$ and $[PPh_4][S_2CN(CH_2)_5]$ reveal charge-separated phosphonium cations and dithiocarbamate anions. The five new crystal structures are used to compare dithiocarbamate bond distances and angles in the presence and absence of arsenic. Nuclear magnetic resonance (NMR) spectra, infrared (IR) spectra, microanalyses, and melting points of the compounds are reported.

1. Introduction

The chemistry of arsenic dithiocarbamates has been investigated since the first half of the 20th century [1–4]. While it is generally understood that dithiocarbamate ligands form robust complexes with arsenic and other "soft" p-block elements (as is often rationalized in terms of Pearson's hard–soft acid–base theory) [5], it is less clear how varying the dithiocarbamate substituents affects As–S bonding and electronic structure. From a broad perspective, As–S bonding is of interest because of its role in arsenic toxicity mechanisms [6], and dithiocarbamate substituents appear to play a significant role in related arsenic binding and distribution in liquid–liquid extraction studies [7]. Our aim is to evaluate the role of dithiocarbamate substituents in $As[S_2CNR_2]_3$ electronic structure using S K-edge X-ray absorption spectroscopy (XAS), which requires a series of dithiocarbamate salts and arsenic complexes with high-purity and well-defined bond metrics. Here we describe the synthesis, characterization and structural comparisons of several new phosphonium and arsenic dithiocarbamate complexes to be used in these efforts [8].

2. Results and discussion

2.1. Synthesis of $[PPh_4][S_2CNR_2]$ and $As[S_2CNR_2]_3$

In preparation for XAS studies, a systematically modified series of $As[S_2CNR_2]_3$ and $[PPh_4][S_2CNR_2]$ complexes were prepared (Scheme 1). These compounds were selected to determine how (1) the orientation of alkyl substituents and (2) the type of substituent (alkyl versus aryl) would affect dithiocarbamate bonding and electronic structure. As reported previously and shown below [9], the ethyl substituents in $S_2CNEt_2^-$ are typically found in a *trans* conformation while the alkyl-substituents in $S_2CN(CH_2)_5^-$ adopt a *cis* conformation that is enforced by the six-membered piperidyl heterocycle.

The salts $[PPh_4][S_2CNR_2]$, where $R_2 = Et_2$ (**1a**), $(CH_2)_5$ (**1b**), and Ph_2 (**1c**), were first prepared so that the bonding and structures of each anion could be evaluated in the absence of arsenic. The non-coordinating tetraphenylphosphonium cation (PPh_4^+) was

* Corresponding author. Tel.: +1 202 994 6934.
E-mail address: srdaly@gwu.edu (S.R. Daly).

http://dx.doi.org/10.1016/j.poly.2014.03.003
0277-5387/

	$[PPh_4][S_2CNR_2]$	$As[S_2CNR_2]_3$
$R_2 = Et_2$	**1a**	**2a**
$R_2 = (CH_2)_5$	**1b**	**2b**
$R_2 = Ph_2$	**1c**	**2c**
$As[S_2CN(CH_2)_5]_2I$	**3**	

Scheme 1. Numbering system used for phosphonium and arsenic dithiocarbamates.

chosen in preference to more traditional alkali metal cations in an effort to minimize intermolecular cation···sulfur interactions that could otherwise interfere with spectroscopic transitions associated with sulfur. In general, the synthesis of $[PPh_4][S_2CNR_2]$ salts are relatively unexplored; only the structure of $[PPh_4][S_2CNMe_2]$ has been reported from crystals obtained adventitiously from a failed reaction [10]. The salts **1a**–**1c** were prepared by metathesis reactions of NaS_2CNR_2 with PPh_4Br in acetonitrile (MeCN). After removal of the solvent and extraction with MeCN, analytically pure **1a**–**1c** could be obtained in high yield by vapor diffusion of diethyl ether (Et_2O) into the MeCN solutions. Large yellow prisms of **1a** and **1b** suitable for single-crystal X-ray diffraction (XRD) were collected and **1c** formed as a yellow microcrystalline solid.

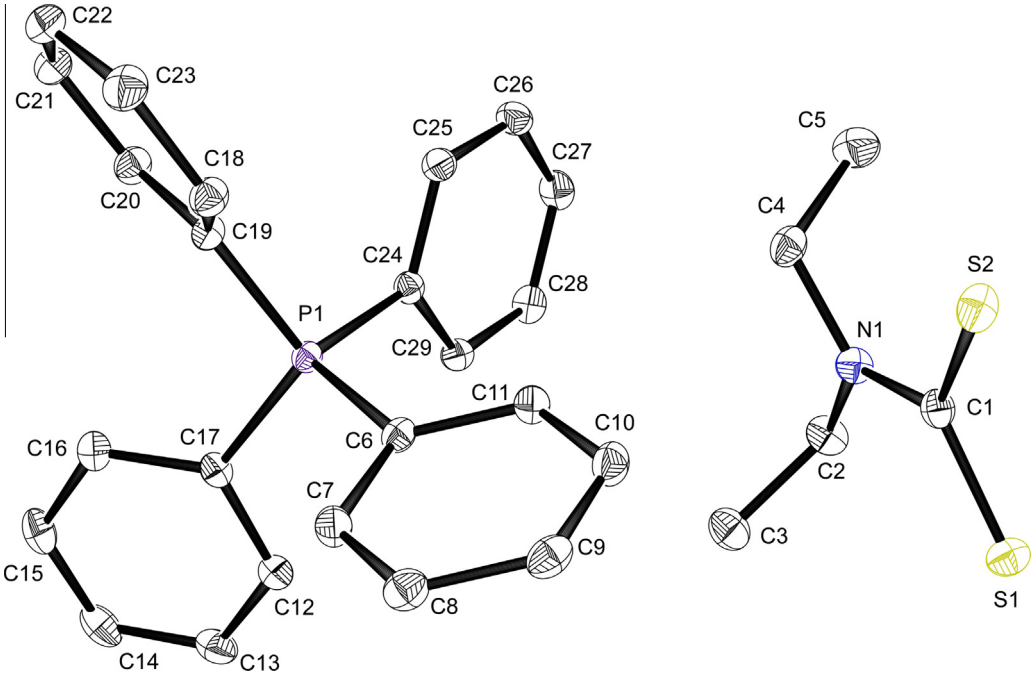

Fig. 1. Molecular structure of $[PPh_4][S_2CNEt_2]$, **1a**. Ellipsoids are drawn at the 50% probability level. Hydrogen atoms have been omitted from the figure.

Table 1
Crystallographic data for $[PPh_4][S_2CNEt_2]$ (**1a**), $[PPh_4][S_2CN(CH_2)_5]$ (**1b**), $As[S_2CN(CH_2)_5]_3$ (**2b**), $As[S_2CNPh_2]_3{\cdot}C_7H_8$ (**2c·C$_7$H$_8$**), and $As[S_2CN(CH_2)_5]_2I$ (**3**).

	1a	**1b**	**2b**	**2c·C$_7$H$_8$**	**3**
Formula	$C_{29}H_{30}NPS_2$	$C_{30}H_{30}NPS_2$	$C_{18}H_{30}N_3S_6As$	$C_{46}H_{38}N_3S_6As$	$C_{12}H_{20}N_2S_4IAs$
FW (g mol^{-1})	487.63	499.64	555.73	849.97	522.36
Crystal system	monoclinic	monoclinic	monoclinic	triclinic	orthorhombic
Space group	$P2_1/c$	$P2_1/c$	$P2_1/c$	$P\bar{1}$	$P2_12_12_1$
a (Å)	13.4423(18)	8.916(5)	17.2691(19)	10.437(4)	6.0207(7)
b (Å)	14.0324(18)	28.434(15)	11.8716(13)	13.306(4)	15.3440(18)
c (Å)	14.3843(19)	10.252(5)	12.1686(14)	16.024(5)	19.444(2)
α (°)	90.00	90.00	90.00	84.200(5)	90.00
β (°)	111.482(2)	99.040(6)	107.589(2)	89.661(5)	90.00
γ (°)	90.00	90.00	90.00	72.601(5)	90.00
V (Å^3)	2524.8(6)	2567(2)	2378.1(5)	2112.0(12)	1796.3(4)
Z	4	4	4	2	4
ρ_{calc} (g cm^{-3})	1.283	1.293	1.552	1.337	1.932
μ (mm^{-1})	0.292	0.289	1.967	1.134	4.068
θ Range (°)	1.63/30.21	2.14/27.80	1.24/30.12	1.613/27.704	1.69/28.36
R(int)	0.0497	0.0443	0.0414	0.0564	0.0669
Data/restraints/parameters	7015/0/298	5952/0/307	6520/0/278	9589/95/505	4462/0/181
Goodness-of-fit (GOF) on F^2	1.038	1.024	1.072	0.985	0.914
R_1 [$I > 2\sigma(I)$][a]	0.0349	0.0350	0.0283	0.0434	0.0298
wR_2 (all data)[b]	0.0940	0.0845	0.0611	0.1040	0.0527
Largest peak and hole (e Å^{-3})	0.0452/−0.338	0.362/−0.282	0.405/−0.508	0.388/−0.378	0.523/−0.450
T (K)	293(2)	120(1)	293(2)	293(2)	293(2)

[a] $R_1 = \sum||F_o| - |F_c||/\sum|F_o|$ for reflections with $F_o^2 > 2\sigma(F_o^2)$.
[b] $wR_2 = [\sum w(F_o^2 - F_c^2)^2/\sum(F_o^2)^2]^{1/2}$ for all reflections.

Table 2
Selected bond distances and angles of phosphonium dithiocarbamates **1a** and **1b**.

Compound	Bond distances (Å)			Bond angles (°)		
	S–C	C–N	N–R	S–C–S	C–N–R	R–N–R
$[PPh_4][S_2CNEt_2]$	1.712(1)	1.359(2)	1.468(2)	121.69(7)	122.2(1)	114.8(1)
(**1a**)	1.722(1)		1.466(2)		123.0(1)	
$[PPh_4][S_2CN(CH_2)_5]$	1.712(2)	1.357(2)	1.470(2)	121.34(9)	124.0(1)	111.5(1)
(**1b**)	1.720(2)		1.462(2)		123.8(1)	

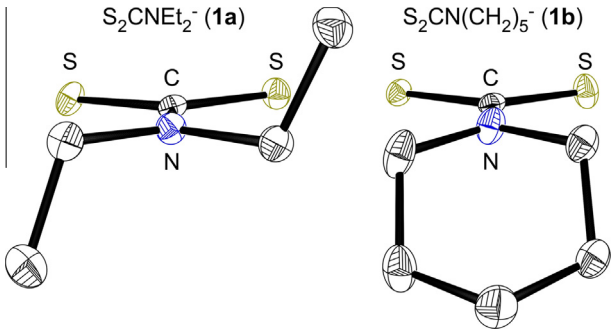

Fig. 2. Comparison of the dithiocarbamate anions $S_2CNEt_2^-$ (left) and $S_2CN(CH_2)_5^-$ (right) from the XRD data of **1a** and **1b**. Ellipsoids are drawn at the 50% probability level. Hydrogen atoms and the tetraphenylphosphonium cations have been omitted from the figure.

The $As[S_2CNR_2]_3$ complexes, where $R_2 = Et_2$ (**2a**), $(CH_2)_5$ (**2b**), and Ph_2 (**2c**), were prepared by treating As_2O_3 or AsI_3 with three equivalents of NaS_2CNR_2. As_2O_3 and AsI_3 can both be used to prepare alkyl-substituted **2a** and **2b** as long as the appropriate solvent is used (aqueous HCl and MeCN, respectively). Attempts to prepare the piperidyl derivative **2b** using AsI_3 and a different solvent (H_2O/EtOH) resulted in a mixture containing a small amount of **2b** and the heteroleptic species $As[S_2CN(CH_2)_5]_2I$ (**3**) (see below). In contrast, a similar reaction with AsI_3 and three equivalents of NaS_2CNPh_2 in H_2O/EtOH yielded $As[S_2CNPh_2]_3$ (**2c**).

It should be clearly noted that **2a** and **2b** have been reported previously [2,11,12], and are only included here to describe a slightly modified version of their synthesis and report the structure of **2b**. Despite the long history of arsenic dithiocarbamate chemistry, phenyl-substituted **2c** has never been described.

2.2. Crystal structures

The structures of the phosphonium salts **1a** and **1b** were determined by single-crystal XRD (Table 1). The structures reveal charge-separated phosphonium cations and dithiocarbamate anions that are free of significant intermolecular cation–anion interactions, as expected given the use of the non-coordinating PPh_4^+ cation (Fig. 1). The closest intermolecular sulfur contacts in **1a** and **1b** involve a phenyl hydrogen atom on PPh_4^+ at 2.79 and 2.83 Å, respectively, which are just within the sum of the van der Waals radii for H and S at 2.89 Å [13,14]. The C–S bond distances in both anions are roughly equivalent at 1.71–1.72 Å, as would be expected for even charge delocalization over both C–S bonds (Table 2). The largest difference between the structures is the aforementioned *trans* versus *cis* orientation of the alkyl substituents (Fig. 2). The enforced six-membered piperidyl ring also causes a decrease in the R–N–R bond angle from 114.8° in $S_2CNEt_2^-$ (**1a**) to 111.5° in $S_2CN(CH_2)_5^-$ (**1b**). The remaining bond angles and distances for **1a** and **1b** are all approximately identical within error.

The molecular structures of $As[S_2CN(CH_2)_5]_3$ (**2b**) and $As[S_2CNPh_2]_3$ (**2c**) are provided in Figs. 3 and 4. As is typical for

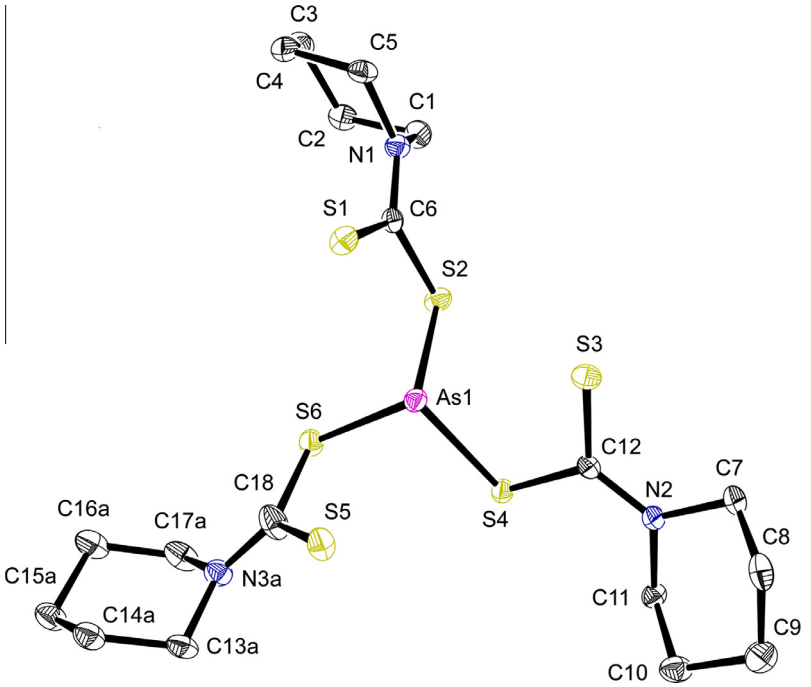

Fig. 3. Molecular structure of $As[S_2CN(CH_2)_5]_3$, **2b**. Ellipsoids are drawn at the 50% probability level. Hydrogen atoms and the disordered component of the piperidyl ring bonded to C18 have been omitted from the figure.

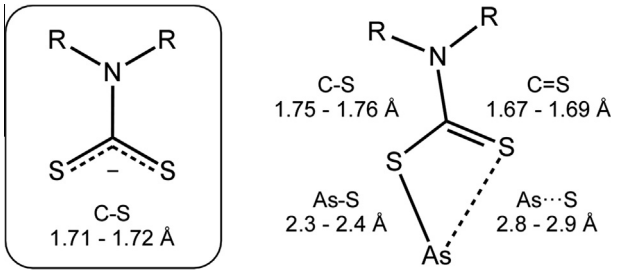

Fig. 4. Comparison of the sulfur bond distances in the structures of $[PPh_4][S_2CNR_2]$ (left) and $As[S_2CNR_2]_3$ (right).

homoleptic arsenic dithiocarbamate complexes, the coordination geometry around each arsenic atom can be described as distorted octahedral with three short As–S bonds (2.32–2.38 Å) forming one triangular face and three long As···S contacts (2.76–2.96 Å) that form the opposite face (Table 3). The longer As···S distances are attributed to steric interactions with the stereoactive lone pair on arsenic [4]. To facilitate the remaining discussion, we will distinguish the two sulfur environments as As–S (bonding) and As···S (close-contact). The S–C bond distances in each dithiocarbamate ligand reflect the different sulfur environments; the sulfur atoms bound to arsenic (As–S) have S–C bond distances of ca. 1.76 Å whereas the As···S sulfur atoms have shorter S–C bond distances that range between 1.67 and 1.69 Å (Fig. 5). The three R–N–R angles in phenyl substituted **2c** are larger than those in **2b** (116–119° versus 112–113°), which reflects the increased steric bulk of the phenyl substituents.

Attempts to prepare **2b** using AsI_3, followed by recrystallization of the reaction precipitate by vapor diffusion of diethyl ether into chloroform solutions, resulted in the formation of a small number

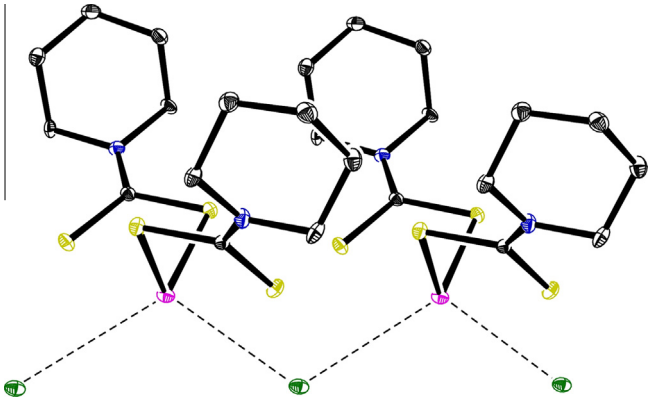

Fig. 5. Extended molecular structure of $As[S_2CN(CH_2)]_2I$, **3**. Ellipsoids are drawn at the 50% probability level. Hydrogen atoms have been omitted from the figure.

of blocks (**2b**) and a large number of brown needles with the composition $As[S_2CN(CH_2)_5]_2I$ (**3**). Single crystal XRD of the needles reveal a coordination polymer with $As[S_2CN(CH_2)_5]_2^+$ fragments that are loosely bridged together by the iodide (Fig. 6). The As–I distances of 3.48 and 3.59 Å are well outside those expected for authenticated terminal As–I single bonds (2.6–2.8 Å) but they fall within the calculated van der Waals distances for As and I (3.83 Å) [13,15,16]. Bridging As–I bonds have precedence for being exceptionally long compared terminal As–I bonds; for example, the dimers $[AsI_2(MeS(CH_2)_2SMe)]2(\mu\text{-}I)_2$ and $[AsI_2\{o\text{-}C_6H_4(AsMe_2)_2\}]_2(\mu\text{-}I)_2$ have bridging As–I distances of 3.34 and 3.43 Å [16,17]. Iodide aside, the coordination environment around each As atom is best described as a distorted see-saw geometry based on the arrangement of the four sulfur atoms. The As–S and S–C bond

Table 3
Selected bond distances and angles for the arsenic dithiocarbamates **2b**, **2c**, and **3**.

	Bond distances (Å)				Bond angles (°)			
$As[S_2CN(CH_2)_5]_3$ (**2b**)	As1–S2	2.3411(5)	S2–C6	1.764(2)	S1–As1–S2	68.39(2)	S3–As1–S4	68.60(2)
	As1–S4	2.3314(5)	S4–C12	1.763(2)	S1–As1–S3	99.79(2)	S3–As1–S5	117.20(1)
	As1–S6	2.3253(5)	S6–C18	1.760(2)	S1–As1–S4	159.14(2)	S3–As1–S6	157.41(2)
	As1–S1	2.8907(5)	S1–C6	1.686(2)	S1–As1–S5	111.28(1)	S4–As1–S5	89.58(2)
	As1–S3	2.8633(5)	S3–C12	1.691(2)	S1–As1–S6	98.34(2)	S4–As1–S6	89.93(2)
	As1–S5	2.9384(6)	S5–C18	1.689(2)	S2–As1–S3	87.82(2)	S5–As1–S6	67.60(2)
	N1–C6	1.334(2)	N2–C7	1.472(2)	S2–As1–S4	93.23(2)	S1–C6–S2	119.1(1)
	N2–C12	1.329(2)	N2–C11	1.472(2)	S2–As1–S5	153.89(2)	S3–C12–S4	117.9(1)
	N3A–C18	1.361(3)	N3A–C13A	1.478(3)	S2–As1–S6	86.43(2)	S5–C18–S6	119.0(1)
	N3B–C18	1.369(6)	N3B–C13B	1.467(8)	C1–N1–C5	111.9(1)	C13–N3B–C17	112.6(5)
	N1–C1	1.475(2)	N3A–C17A	1.478(4)	C7–N2–C11	112.9(1)	C13–N3A–C17	112.6(2)
	N1–C5	1.473(2)	N3B–C17B	1.476(8)				
$As[S_2CNPh_2]_3$ (**2c**)	As1–S1	2.334(1)	S1–C1	1.751(3)	S1–As1–S2	70.23(3)	S4–As1–S5	114.94(3)
	As1–S3	2.333(1)	S3–C2	1.755(3)	S1–As1–S3	93.38(3)	S4–As1–S6	110.94(3)
	As1–S5	2.383(1)	S5–C3	1.748(3)	S1–As1–S4	149.17(3)	S5–As1–S6	67.15(3)
	As1–S2	2.763(1)	S2–C1	1.680(3)	S1–As1–S5	87.70(3)	S1–C1–S2	118.7(2)
	As1–S4	2.95(1)	S4–C2	1.678(3)	S1–As1–S6	96.74(3)	S3–C2–S4	121.9(2)
	As1–S6	2.958(1)	S6–C3	1.669(3)	S2–As1–S3	89.48(3)	S5–C3–S6	121.9(2)
	C11–N1	1.452(3)	C1–N1	1.345(4)	S2–As1–S4	84.75(3)	C11–N1–C21	119.0(2)
	C21–N1	1.457(4)	C2–N2	1.347(3)	S2–As1–S5	157.70(3)	C31–N2–C41	116.2(2)
	C31–N2	1.449(4)	C3–N3	1.355(3)	S2–As1–S6	117.25(3)	C51–N3–C61	115.7(2)
	C41–N2	1.448(3)			S3–As1–S4	67.95(3)		
	C51–N3	1.450(4)			S3–As1–S5	88.66(3)		
	C61–N3	1.453(4)			S3–As1–S6	153.24(3)		
$As[S_2CN(CH_2)_5]_2I$ (**3**)	As1–S1	2.302(1)	S1–C6	1.749(4)	S1–As1–S2	74.45(4)	S1–As1–I1	80.80(4)
	As1–S4	2.303(1)	S4–C12	1.744(4)	S3–As1–S1	88.00(4)	S2–As1–I1	126.34(4)
	As1–S2	2.496(1)	S2–C6	1.715(4)	S1–As1–S4	97.27(4)	S3–As1–I1	70.18(3)
	As1–S3	2.512(1)	S3–C12	1.707(4)	S3–As1–S2	151.93(4)	S4–As1–I1	144.25(4)
	As1–I1	3.5906(8)	N1–C3	1.478(5)	S4–As1–S2	86.37(4)	S2–C6–S1	114.1(2)
	As1–I1a[a]	3.479(1)	N1–C4	1.470(5)	S3–As1–S4	74.08(3)	S3–C12–S4	114.7(2)
	N1–C6	1.314(4)	N2–C9	1.473(5)	C3–N1–C4	113.2(4)		
	N2–C12	1.329(5)	N2–C11	1.470(5)	C9–N2–C11	113.8(4)		

[a] Symmetry transformation used to generate equivalent atoms: $a = x + 1, y, z$.

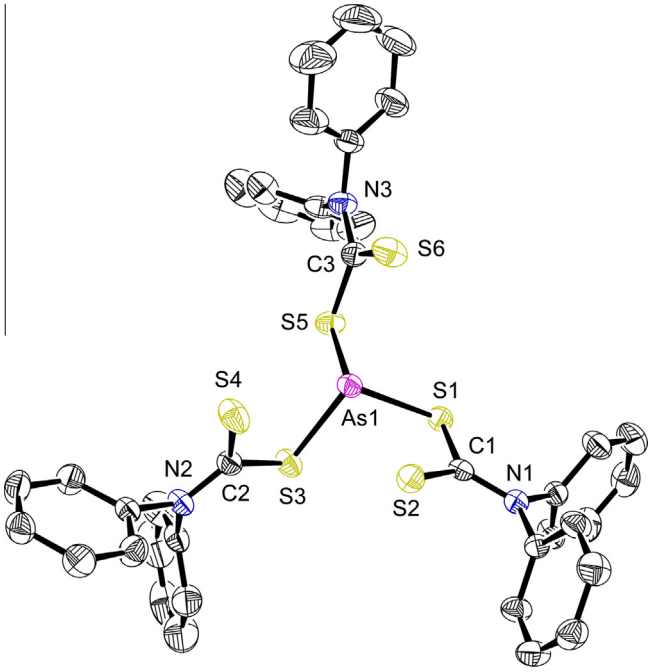

Fig. 6. Molecular structure of $As[S_2CNPh_2]_3 \cdot C_7H_8$, **2c**·$\mathbf{C_7H_8}$. Ellipsoids are drawn at the 35% probability level. The toluene solvate and the hydrogen atoms have been omitted from the figure.

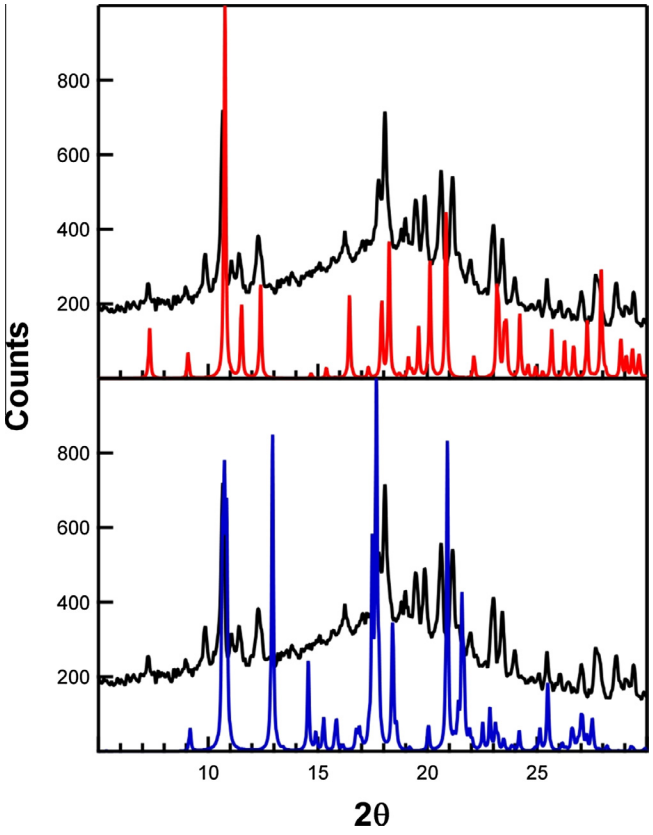

Fig. 7. Experimental powder XRD pattern of the precipitate obtained from the reaction of AsI_3 and three equivalents of $NaS_2CN(CH_2)_5$ (black). *Top* – comparison with the calculated powder XRD pattern from the single crystal diffraction data for **3** (red). *Bottom* – comparison with the calculated powder XRD pattern from the single crystal diffraction data for **2b** (blue). (Color online.)

distances in each ligand do not deviate as much as those in **2b**. There is a 0.2 Å difference between the As–S bonds in each ligand (versus >0.4 Å in **2b**) and all four S–C bonds fall within the range of 1.71–1.75 Å. Overall the structure of heteroleptic $As[S_2CNR_2]_2I$ complexes are relatively rare. While the synthesis of **3** and other $As[S_2CNR_2]_2I$ complexes have been reported [18], only one other structure is known [19].

Given that the reaction of AsI_3 with three equivalents of $NaS_2CN(CH_2)_5$ yielded crystals of **3** and **2b**, we analyzed the crude reaction precipitate by powder XRD to evaluate the relative proportion of each compound in the mixture. The powder XRD data is presented in Fig. 7 with the calculated powder XRD pattern of **2b** (top) and **3** (bottom) from the single crystal diffraction data for comparison. The data indicates that the major product in the reaction precipitate is the mixed iodide complex **2b**. The incomplete metathesis in H_2O/EtOH solutions contrasts the reaction behavior reported for AsI_3 and sodium dialkyldithiocarbamates in MeCN. For example, it was reported that the reaction of AsI_3 with three equivalents of NaS_2CNEt_2 in MeCN yielded $As[S_2CNEt_2]_3$ in 79% yield [9]. The difference in the AsI_3 metathesis chemistry between EtOH/H_2O and MeCN reaction solvents appears to result from differences in solubility: $As[S_2CN(CH_2)_5]_2I$ precipitates from EtOH/H_2O before the metathesis is complete whereas all arsenic-containing species remain soluble in MeCN.

2.3. Spectroscopic analysis

All seven compounds were characterized by NMR spectroscopy. The ^1H and ^{31}P NMR spectra of the phosphonium salts **1a**–**1c** were collected in CD_3CN and the ^1H NMR spectra of the arsenic dithiocarbamates **2a**–**2c** and **3** were collected in $CDCl_3$. In general, the proton spectra of the phosphonium salts are unexceptional and exhibit peak splittings and integrations that reflect each of the dithiocarbamate anions. Similar to data obtained on tetraphenylphosphonium dithiophosphinates [20], the proton NMR spectra of **1a**–**1c** reveal multiplets for the PPh_4^+ cation between $\delta = 7.65$ and 7.94 and a complimentary singlet is observed in the $^{31}P\{^1H\}$ NMR spectra at $\delta = 24.4$. The arsenic dithiocarbamates exhibit similar ^1H NMR shifts as their phosphonium analogs and the NMR shifts for **2a** and **2b** closely match those reported previously in units of τ [12,21]. The spectrum of **2a** reveals a triplet at $\delta = 1.29$ and a quartet at $\delta = 3.88$ for the methyl and methylene protons, and the lack of additional peaks is consistent with retention of the C_3 symmetry in solution. The proton NMR spectrum of **2b** also yields two peaks despite having three unique proton environments in the piperidyl substituents. The peaks appear as broadened singlets at $\delta = 1.69$ and 4.05 (6:4 ratio) compared to the three resonances at $\delta = 1.49$, 1.60, and 4.38 (4:2:4 ratio) in the proton NMR spectrum of **1b**. The peak broadening and coalescence of three peaks to two in the spectrum of **2b** can likely be attributed to different conformations of the six-membered piperidyl ring within each ligand. As observed for $As[S_2CN(CH_2)_5]_3$, the proton NMR spectrum of $As[S_2CN(CH_2)_5]_2I$ (**3**) also exhibits two broad singlets but with slightly different shifts than **2b** at $\delta = 1.75$ and 3.93. The presence of only two peaks indicates that the two unique dithiocarbamate environments observed in the solid-state are equivalent in solution on the NMR timescale.

IR data were collected on the phosphonium salts **1a**–**1c** and on the complimentary arsenic complexes **2a** – **2c**. It is generally agreed that the C–NR_2 stretches and C–S stretches for dithiocarbamates typically fall in the range of 1400–1500 and 930–1030 cm^{-1}, respectively [4,22]. Overall, the spectra of **1a**–**1c** are strikingly similar, which can be attributed in part to the tetraphenylphosphonium cation that is common to all three salts. Identical peaks, however, are also observed in the C–NR_2 and C–S stretching regions for all three compounds at 1434, 1458 and 1480 cm^{-1} and at 948, 970, and 994 cm^{-1}, respectivly. Despite the localization of

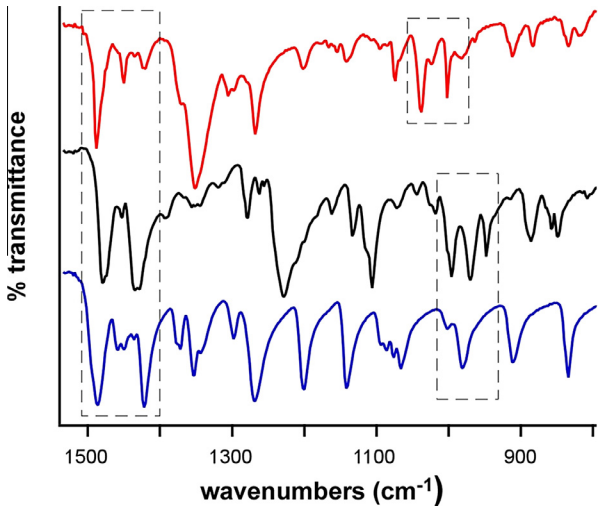

Fig. 8. Comparison of the IR spectra for $As[S_2CNEt_2]_3$ (bottom; blue), $As[S_2CN(CH_2)_5]_3$ (middle; black), and $As[S_2CNPh_2]_3$ (top; red). The assigned C–S and C–NR_2 stretching regions and peaks are emphasized with the dashed boxes. (Color online.)

C–S bonds in the structures of the arsenic dithiocarbamates, the IR peaks in the spectra of **2a**–**2c** do not change much except for those assigned to C–S stretching bands in $As[S_2CNPh_2]_3$. The alkyl-substituted **2a** and **2b** exhibit strong peaks between 970 and 1002 cm^{-1} that compare well to ν(CS) peaks previously reported [12,21], but these appear to shift to higher energy in the spectrum of **2c** at 1002, 1022 and 1034 cm^{-1} (Fig. 8). Given the change in substituents from alkyl to aryl, the unique shift in the C–S stretching frequencies for **2c** is likely attributed to the addition of π-conjugation between the phenyl substituents and the π-orbitals delocalized over carbon, nitrogen and sulfur. The higher energy shift indicates an increase in C–S double-bond character, which is consistent with increased π-mixing with phenyl.

3. Conclusion

In summary, we have reported the synthesis and characterization of $As[S_2CNPh_2]_3$ and several new tetraphenylphosphonium dithiocarbamates. The $[PPh_4][S_2CNR_2]$ salts have the qualities desired for spectroscopic analysis; they can be prepared in high purity and the structures of $[PPh_4][S_2CNEt_2]$ and $[PPh_4][S_2CN(CH_2)_5]$ reveal a lack of appreciable intermolecular cation–sulfur interactions. In total, five new crystal structures have been reported, and these have provided important structural metrics needed to support spectroscopic comparisons of dithiocarbamates in the presence and absence of arsenic. Varying the substituents attached to nitrogen does not appear to impart significant changes in $As[S_2CNR_2]_3$ bond distances and angles, but a clear difference is observed in the C–S stretching region when alkyl substituents in **2a** and **2b** are changed to phenyl in **2c**. The IR results suggested that the dithiocarbamate substituents do affect sulfur bonding when bound to arsenic, and future reports will describe S K-edge X-ray absorption spectroscopy (XAS) efforts aimed at quantifying these contributions as they pertain to $As[S_2CNR_2]_3$ electronic structure and As–S bonding.

4. Experimental

4.1. General considerations

Unless specified otherwise, all reactions were performed in air. The dithiocarbamate salts $NaS_2CN(CH_2)_5$ and NaS_2CNPh_2 were prepared according to literature methods [7,23]. AsI_3 (Alfa Aesar), As_2O_3 (Mallinckrodt), PPh_4Br (Acros), $NaS_2CNEt_2{\cdot}3H_2O$ (Mallinckrodt), and conc. HCl (Fisher) were used as received. Solvents were purchased from commercial vendors and used as received. H_2O was purified to 18.2 MW-cm resistivity using a Siemens LoboStar UV2 ultra-pure water purification system.

Elemental analyses were carried out by Midwest MicroLab, LLC (Indianapolis, IN). The infrared spectra were recorded on a Perkin-Elmer Frontier FTIR Spectrometer using an attenuated total reflectance (ATR) sampling accessory. The ^1H and ^{31}P NMR data were obtained using an Agilent NMR spectrometer at 400 and 121 MHz, respectively. Chemical shifts are reported in δ units (positive shifts to high frequency) relative to TMS (^1H) and H_3PO_4 (^{31}P). Melting points were determined in open capillaries on a Thomas-Hoover Unimelt apparatus.

4.2. $[PPh_4][S_2CNEt_2]$, (**1a**)

To a mixture of $NaS_2CNEt_2{\cdot}3H_2O$ (0.215 g, 0.954 mmol) and PPh_4Br (0.403 g, 0.961 mmol) was added MeCN (5 mL). The mixture was stirred for 30 min, which yielded a yellow solution and a white precipitate. The mixture was evaporated to dryness under vacuum. MeCN (3 mL) was added to the solid residue and the mixture was filtered into a 20 mL scintillation vial. Yellow crystals of **1a** were grown over the course of a week by vapor diffusion with diethyl ether (20 mL). Yield: 0.374 g (80.4%). Mp: 176–177 °C *Anal.* Calc.: C, 71.43; H, 6.2; N, 2.87; S, 13.15. Found: C, 71.20; H, 6.14; N, 2.82; S, 12.70%. ^1H NMR (CD_3CN, 25 °C): δ 1.16 (t, CH_3, 6H), 4.10 (q, NCH_2, 4H), 7.65–7.77 (m, PPh_4, 16H), 7.90–7.94 (m, PPh_4, 4 H). $^{31}P\{^1H\}$ NMR (CD_3CN, 25 °C): δ 24.4 (s, PPh_4). IR (cm^{-1}): 606 w, 616 w, 648 w, 686 vs 720 vs 750 m, 758 m, 810 w, 840 w, 850 w, 882 m, 900 w, 916 w, 936 w, 948 w, 970 m, 994 m, 1024 w, 1044 w, 1068 w, 1104 vs 1108 m, 1158 w, 1200 m, 1208 m, 1242 m, 1276 w, 1318 w, 1340 w, 1360 w, 1390 m, 1434 s, 1458 w, 1480 m, 1584 w, 2846 w, 2938 w, 2988 w, 3036 w.

4.3. $[PPh_4][S_2CN(CH_2)_5]$, (**1b**)

Prepared as described for **1a** with PPh_4Br (0.410 g, 0.978 mmol) and $NaS_2CN(CH_2)_5$ (0.229 g, 0.965 mmol). Yield: 0.313 g (64.9%). Mp: 174–175 °C. *Anal.* Calc.: C, 72.11; H, 6.20; N, 2.80; S, 12.83. Found: C, 71.97; H, 6.00; N, 2.86; S, 13.21%. ^1H NMR (CD_3CN, 25 °C): δ 1.49 (m, 4H), 1.60 (m, 2H), 4.38 (vt, NCH_2, 4H), 7.65–7.77 (m, PPh_4, 16H), 7.89–7.94 (m, PPh_4, 4H). $^{31}P\{^1H\}$ NMR (CD_3CN, 25 °C): δ 24.4 (s, PPh_4). IR (cm^{-1}): 606 w, 6116 w, 686 vs 720 vs 752 m, 758 vm, 810 w, 850 w, 882 m, 934 w, 948 m, 970 s, 994 m, 1022 w, 1068 w, 1106 s, 1118 m, 1158 w, 1200 m, 1208 m, 1240 m, 1276 w, 1318 w, 1340 w, 1358 w, 1390 m, 1434 s, 1458 w, 1480 m, 1584 w, 2846 w, 2936 w, 2988 w, 3036 w.

4.4. $[PPh_4][S_2CNPh_2]$, (**1c**)

Prepared as described for **1a** with PPh_4Br (0.31 g, 0.75 mmol) and NaS_2CNPh_2 (0.20 g, 0.75 mmol). Mp: 130–131 °C. *Anal.* Calc.: C, 76.13; H, 5.18; N, 2.40; S, 10.99. Found: C, 75.71; H, 5.15; N, 2.40; S, 10.87%. ^1H NMR (CD_3CN, 25 °C): δ 7.05–7.09 (m, Ph_2, 2H), 7.20–7.25 (m, Ph_2, 4H), 7.30–7.33 (m, Ph_2, 4H), 7.65–7.77 (m, PPh_4, 16H), 7.89–7.94 (m, PPh_4, 4H). ^{31}P NMR (CD_3CN, 25 °C): δ 24.4 (s, PPh_4). IR (cm^{-1}): 604 w, 616 w, 686 w, 718 vs 750 m 758 m, 810 w, 850 w, 882 m, 900 w, 934 w, 948 m, 970 m, 994 m, 1024 w, 1044 w, 1068 w, 1106 s, 1118 m, 1158 w, 1200 m, 1208 m, 1242 m, 1276 w, 1316 w, 1340 w, 1358 w, 1390 m, 1434 s, 1458 w, 1482 w, 1584 w, 1480 m, 1584 w, 2846 w, 2938 w, 2988 w, 3038 w.

4.5. As[S_2CNEt_2]$_3$, (**2a**)

Prepared with slight modification of a known procedure [24]. To a solution of NaS_2CNEt_2 (1.371 g, 6.06 mmol) in water (10 mL) was added a solution of As_2O_3 (0.201 g, 1.02 mmol) in concentrated hydrochloric acid (5 mL). A thick yellow precipitate formed and the mixture was stirred for 1 h. The solid was collected by filtration and light green crystals were obtained after recrystallization from chloroform. Yield: 0.65 g (61%). Mp: 139–140 °C. *Anal.* Calc.: C, 34.66; H, 5.82; N, 8.08; S, 37.02. Found: C, 34.68; H, 6.03; N, 8.06; S, 36.66%. ^{1}H NMR ($CDCl_3$, 25 °C): δ 1.29 (t, CH_3, 18H), 3.88 (q, CH_2, 12H). IR (cm^{-1}): 600 w, 776 m, 834 s, 912 m, 982 m, 1002 w, 1066 m, 1076 m, 1086 m, 1094 m, 1142 s, 1200 s, 1270 vs 1298 w, 1354 m, 1372 m, 1422 vs 1450 m, 1458 m, 1486 vs 2868 w, 2932 w, 2972 w.

4.6. As[$S_2CN(CH_2)_5$]$_3$, (**2b**)

Prepared as described for **2a** using $NaS_2CN_2(CH_2)_5$ and As_2O_3. Mp: 228–229 °C. *Anal.* Calc.: C, 38.90; H, 5.44; N, 7.56; S, 34.62. Found: C, 38.87; H, 5.75; N, 7.48; S, 34.19. ^{1}H NMR ($CDCl_3$, 25 °C): δ 1.69 (br s, 18H), 4.05 (br s, 12H). IR (cm^{-1}): 602 m, 616 w, 646 w, 688 m, 720 m, 758 w, 808 w, 848 m, 858 m, 886 m, 948 s, 970 s, 996 s, 1018 w, 1044 w, 1072 w, 1106 vs 1134 m, 1162 w, 1228 vs 1256 w, 1262 w, 1280 m, 1320 w, 1352 w, 1428 s, 1434 s, 1453 w, 1474 sh, 1480 s, 1584 w, 2850 m, 2938 m, 2982 w, 3038 w.

4.7. As[S_2CNPh_2]$_3$, (**2c**)

To a suspension of AsI_3 (0.142 g, 0.312 mmol) in a 1:1 solution of ethanol and deionized water (20 mL) was added a solution of NaS_2CNPh_2 (0.302 g, 0.927 mmol) in deionized water (10 mL). A thick off-white precipitate formed and the mixture was heated to 50 °C for 2 h. The mixture was cooled to room temperature and filtered. The solid was allowed to dry in air overnight. To the solid was added to 120 mL of toluene and the mixture was heated to reflux to completely dissolve the solid. The yellow solution was slowly cooled to RT and then stored at 4 °C. Yellow prisms formed overnight. The collected crystals were exposed to dynamic vacuum for 30 min to remove the toluene solvate in the crystal lattice. Yield: 0.070 g (28%). Mp: > 250 °C. *Anal.* Calc.: C, 57.97; H, 3.74; N 5.20; S, 23.81. Found: C, 58.28; H, 3.76; N, 4.99; S, 22.83%. ^{1}H NMR ($CDCl_3$, 25 °C): δ 7.31–7.49 (m). IR (cm^{-1}): 624 m, 630 w, 646 m, 668 w, 688 m, 698 s, 746 m, 752 m, 776 w, 818 w, 834 w, 884 w, 912 w, 982 w, 1002 m, 1022 m, 1034 s, 1074 m, 1096 w, 1142 w, 1154 w, 1202 w, 1268 m, 1290 m, 1306 m, 1332 sh, 1347 vs 1450 w, 1488 s, 1588 w, 2870 w, 2972 w, 3050 w.

4.8. As[$S_2CN(CH_2)_5$]$_2$I, (**3**)

To a suspension of AsI_3 (0.252 g, 0.553 mmol) in a 1:1 solution of ethanol and deionized water (20 mL) was added a solution of $NaS_2CN(CH_2)_5$ (0.339 g, 1.85 mmol) in deionized water (10 mL), as described for the preparation of **2c**. A white precipitate immediately formed and the mixture was stirred for 15 min. The mixture was filtered and the solid was dissolved in chloroform. Vapor diffusion of diethyl ether into the chloroform solution over several days resulted in the formation of brown needles (**3**; major product) and blocks (**2b**; minor product). The crystallized yield of **3** was low (~30 mg), but was sufficient to obtain the following data: *Anal.* Calc.: C, 27.59; H, 3.86; N5.36; I, 24.29. Found: C, 26.98; H, 3.70; N, 5.11; I, 23.91%. ^{1}H NMR ($CDCl_3$, 25 °C): δ 1.75 (br s, 12H), 3.93 (br s, 8H). Powder XRD of the precipitate from an identical synthetic prep indicated that the major product was **3**.

4.9. Crystallographic details

Single crystals of **1a** and **1b** were obtained by vapor diffusion of diethyl ether into acetonitrile solutions and were mounted in a nylon cryoloop or MiTeGen mount with Paratone-N oil in air. The data were collected on a Bruker diffractometer with an APEX II charge-coupled-device (CCD) detector. Data for **1b** were collected at 120 K using a Cryo industries of America G2 low temperature device. All other data were collected at room temperature. Single crystals of **2b** and **3**, obtained by vapor diffusion of diethyl ether into chloroform solutions, were treated identically, as were single crystals of **2c** obtained from toluene. The instrument was equipped with graphite monochromatized Mo Kα X-ray source (λ = 0.71073 Å) with monocapillary optics. Data collection and initial indexing and cell refinement were handled using APEX II software [25]. Frame integration, including Lorentz-polarization corrections, and final cell parameter calculations were carried out using SAINT+ software [26]. The data were corrected for absorption using redundant reflections and the SADABS program [27]. The structure was solved using direct methods and difference Fourier techniques. All hydrogen atom positions were idealized, and were allowed to ride on the attached carbon atoms. The final refinement included anisotropic temperature factors on all non-hydrogen atoms. Data collection and refinement details are listed in Table 1.

Powder XRD of the bulk precipitate obtained from the reaction of AsI_3 with three equivalents of Na[$S_2CN(CH_2)_5$] were collected on Rigaku Miniflex II equipped with a Cu Kα X-ray source. Scans were collected from 2θ = 3–60° at a scan speed of 2° per minute and a sampling width of 0.020°. The power was set to 15 kV and 30 mA.

Acknowledgements

Funding for this work was provided by the George Washington University. Los Alamos National Laboratory is operated by Los Alamos National Security, LLC, for the National Nuclear Security Administration of U.S. Department of Energy under Contract DEAC52-06NA25396. We would like to thank the Cahill Group at GW, especially Gian Surbella and Andrew Kerr, for their assistance collecting portions of the XRD data.

Appendix A. Supplementary data

CCDC 973372, 973373, 973374, 973375, 973376 contain the supplementary crystallographic data for compounds **1a**, **1b**, **2b**, **2c**, and **3**, respectively. These data can be obtained free of charge via http://www.ccdc.cam.ac.uk/conts/retrieving.html, or from the Cambridge Crystallographic Data Centre, 12 Union Road, Cambridge CB2 1EZ, UK; fax: +44 1223-336-033; or e-mail: deposit@ccdc.cam.ac.uk.

References

[1] L. Malatesta, Gazz. Chim. Ital. 69 (1939) 629.
[2] L. Bourgeois, J. Bolle, Meml. Serv. Chim. l'Etat 34 (1948) 411.
[3] S.S. Garje, V.K. Jain, Coord. Chem. Rev. 236 (2003) 35.
[4] P.J. Heard, Prog. Inorg. Chem. 53 (2005) 1.
[5] R.G. Pearson, J. Am. Chem. Soc. 85 (1963) 3533.
[6] S. Shen, X.-F. Li, W.R. Cullen, M. Weinfeld, X.C. Le, Chem. Rev. 113 (2013) 7769.
[7] B. Ballard, D. Wycoff, E.R. Birnbaum, K.D. John, J.W. Lenz, S.S. Jurisson, C.S. Cutler, F.M. Nortier, W.A. Taylor, M.E. Fassbender, Appl. Radiat. Isot. 70 (2012) 595.
[8] XAS results will be described in a separate report.
[9] F. Li, H.D. Yin, J. Zhai, D.Q. Wang, Acta Crystallogr., Sect. E 62 (2006) m2205.
[10] M. Draganjac, D. Minick, E.M. Holt, Proc. Ark. Acad. Sci. 44 (1990) 35.
[11] M. Colapietro, A. Domenicano, L. Scaramuzza, A. Vaciago, Chem. Commun. (1968) 302.
[12] G.E. Manoussakis, P. Karayannidis, J. Inorg. Nucl. Chem. 31 (1969) 2978.
[13] A. Bondi, J. Phys. Chem. 68 (1964) 441.

[14] R.S. Rowland, R. Taylor, J. Phys. Chem. 100 (1996) 7384.
[15] R. Kniep, H.D. Reski, Inorg. Chim. Acta 64 (1982) L83.
[16] N.J. Hill, W. Levason, G. Reid, Inorg. Chem. 41 (2002) 2070.
[17] N.J. Hill, W. Levason, G. Reid, J. Chem. Soc. Dalton Trans. (2002) 1188.
[18] C.A. Tsipis, G.E. Manoussakis, Inorg. Chim. Acta 18 (1976) 35.
[19] H.-D. Yin, F. Li, Wuji Huaxue Xuebao 23 (2007) 451.
[20] S.R. Daly, J.R. Klaehn, K.S. Boland, S.A. Kozimor, M.M. MacInnes, D.R. Peterman, B.L. Scott, Dalton Trans. 41 (2012) 2163.
[21] G.E. Manoussakis, C.A. Tsipis, J. Inorg. Nucl. Chem. 35 (1973) 743.
[22] H.L.M. Van Gaal, J.W. Diesveld, F.W. Pijpers, J.G.M. Van der Linden, Inorg. Chem. 18 (1979) 3251.
[23] R. Sharma, N.K. Kaushik, J. Therm. Anal. Calorim. 78 (2004) 953.
[24] J.S. Ashford, P. Gould, Organo-arsenic compounds. G.B. Patent 1,080,892. August 23, 1967.
[25] APEX II 1.08, Bruker AXS Inc, Madison, Wisconsin 53719.
[26] SAINT+ 7.06, Bruker AXS Inc, Madison, Wisconsin 53719.
[27] SADABS 2.03, George Sheldrick, University of Göttingen, Germany.